Articles

Structural Characterization of the 1:1 Adduct Formed between the Antitumor Antibiotic Hedamycin and the Oligonucleotide Duplex d(CACGTG)$_2$ by 2D NMR Spectroscopy†

Spiro Pavlopoulos,‡ Wendy Bicknell,‡ David J. Craik,*,§ and Geoffrey Wickham*,||

Department of Medicinal Chemistry, Victorian College of Pharmacy, Monash University, Melbourne, Victoria, Australia, Centre for Drug Design and Development, University of Queensland, Brisbane, Queensland, Australia, and Department of Chemistry, University of Wollongong, Wollongong, New South Wales, Australia

Received October 25, 1995; Revised Manuscript Received May 2, 1996⊗

ABSTRACT: 2D NMR spectroscopic methods have been used to determine the structure of the adduct formed between the antitumor antibiotic hedamycin and the oligodeoxyribonucleotide duplex d(CACGTG)$_2$. Evidence for both intercalation and alkylation in the adduct was observed, and a model for the binding interaction was constructed based on intermolecular NOEs and distance-restrained molecular dynamics. In our computationally refined model, the anthrapyrantrione chromophore of hedamycin is intercalated between the 5′-CG-3′ bases with the two aminosugar groups placed in the minor groove and the six carbon bisepoxide side chain located in the major groove. The anglosamine sugar attached at C8 is oriented in the 3′ direction relative to the intercalation site, while the *N*,*N*-dimethylvancosamine attached at C10 is oriented to the 5′ side, with each aminosugar wedged between a guanine exocyclic amino group and one of the groove walls. The terminal epoxide carbon C18 is covalently bound to the N7 atom of the central guanine, as evidenced by lability of the C8 hydrogen of this purine upon reaction with hedamycin. Our binding model places the C10-attached *N*,*N*-dimethylvancosamine of hedamycin in van der Waals contact with the alkylated strand. A strong NOE contact verifies the close proximity of the terminal methyl group (C19) of the bisepoxide side chain to the methyl group of the thymine on the 3′ side of the alkylated guanine. This, in conjunction with other data, suggests hydrophobic interactions between the bisepoxide chain and the floor of the major groove may contribute to sequence recognition. Furthermore, it is proposed that the 5′-CGT sequence selectivity of hedamycin arises, in part, from complementarity in shape between the chromophore substituents and the major and minor groove at the binding site.

Hedamycin (Figure 1) is a naturally occurring antitumor antibiotic which alkylates double-stranded DNA in a highly sequence selective manner (Murray et al., 1995; Prakash et al., 1995; Sun et al., 1995). It is a member of the pluramycin class of antitumor antibiotics and consists of a planar anthrapyrantrione chromophore to which is attached two aminosugar rings at one end and a bisepoxide-containing side chain at the other end. Unlike simple DNA alkylating agents, such as nitrogen mustard, which react preferentially at guanines located in runs of consecutive guanines, hedamycin and other intercalating alkylators (Wickham et al., 1991; Murray et al., 1996) show a high affinity for certain isolated guanine bases. In the case of hedamycin, the sequence selectivity is 5′-pyGT, with 5′-CGT sites favored over 5′-TGT sites. We are interested in establishing the structural

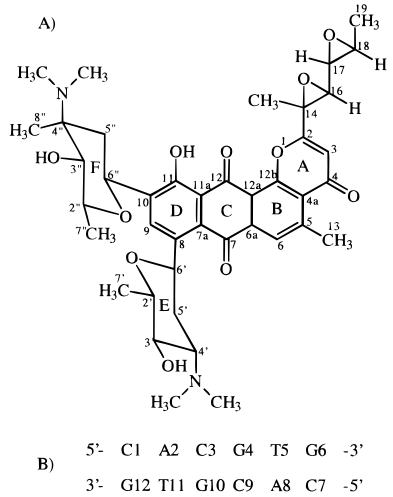

FIGURE 1: (A) Chemical structure and numbering scheme of hedamycin. (B) Numbering scheme of the complexed oligonucleotide duplex.

† This work was supported by the National Health and Medical Research Council of Australia.

* Corresponding authors: Dr. Geoffrey Wickham, Chemistry Department, University of Wollongong, Northfields Ave., Wollongong, NSW, Australia 2522. Telephone: 61-42-214 418. Fax: 61-42-214 287. E-mail: g.wickham@uow.edu.au. Professor David Craik, NMR Laboratory, Centre for Drug Design and Development, University of Queensland, Brisbane, Queensland, Australia 4072. Telephone: 61-7-3365 4945. Fax: 61-7-3365 2487. E-mail: d.craik@mailbox.uq.oz.au.

‡ Monash University.

§ University of Queensland.

|| University of Wollongong.

⊗ Abstract published in *Advance ACS Abstracts,* June 15, 1996.

basis for the DNA sequence selectivity exhibited by hedamycin and have employed mass spectrometry and NMR spectroscopy to achieve this goal. In recent reports, we described the novel use of electrospray mass spectrometry to probe the interaction of hedamycin with the hexadeoxyribonucleotide duplexes $d(CACGTG)_2$ and $d(CGTACG)_2$ (Wickham et al., 1995a,b). The mass spectral studies provided direct evidence for guanine alkylation by hedamycin (G. Wickham et al., unpublished results) and, also, confirmed the significant increase in duplex stability upon ligand binding. In other recent work, NMR titration experiments involving two 5′-CGT-3′-containing oligonucleotides have provided evidence for reversible, intercalative, DNA binding by hedamycin prior to purine alkylation (S. Pavlopoulos et al., unpublished results). The titration experiments also verified the preference of hedamycin for 5′-CG over 5′-TG sites.

In this paper, we describe details of the three-dimensional structure of hedamycin bound to the oligonucleotide duplex $d(CACGTG)_2$, as determined by 2D NMR spectroscopy and restrained molecular modeling. During the preparation of this paper, NMR studies of the pluramycin-like compound altromycin B bound to $d(GAAGTACTTC)_2$ and of hedamycin bound to the oligonucleotide duplex $d(GATGTACATC)_2$ were published in which structural factors governing sequence selectivity were discussed (Hansen et al., 1995; Hansen & Hurley, 1995). In the model of the 2:1 hedamycin−DNA adduct determined by Hurley and co-workers, the anthrapyran chromophores of the ligands thread the double helix and intercalate to the 5′ side of the alkylated guanines, which are both 5′-TGs. The terminal epoxide carbon (C18) is bound to the N7 of guanine in the major groove, and the C8 and C10 sugars occupy the minor groove, with the anglosamine attached at C8 oriented in the 3′ direction relative to the intercalation site and the *N*,*N*-dimethylvancosamine attached at C10 oriented to the 5′ side. Altromycin B, which has no sugar attached at C8 of the anthrapyran chromophore, an altrose unit attached at C5, and only a four carbon monoepoxide side chain, also threads the double helix and alkylates the N7 of guanine.

While Hurley and co-workers have structurally characterized the 5′-TG sequence selectivity of hedamycin, our study is concerned with binding to the higher affinity 5′-CG sequence. The effect of an additional NH_2 group in the minor groove resulting from the presence of a cytosine in place of a thymine (i.e., 5′-CG versus 5′-TG) is discussed, and, in addition, we have attempted to identify the relevance of the thymine located to the 3′ side of the alkylated guanine at a high affinity 5′-CGT binding site. The hedamycin binding model proposed in this paper is in broad agreement with that reported by Hansen et al. (1995).

MATERIALS AND METHODS

Sample Preparation. The hedamycin sample used in this study was generously donated by the Bristol-Myers Co. Synthesis of the oligonucleotide duplex $d(CACGTG)_2$ and preparation of the hedamycin:$d(CACGTG)_2$ adduct will be described elsewhere (S. Pavlopoulos et al., unpublished data). Solutions of hedamycin, $d(CACGTG)_2$, and the hedamycin−$d(CACGTG)_2$ adduct in D_2O contained 50 mM NaCl, 6 mM NaH_2PO_4, and 4 mM Na_2HPO_4 (pH 6.7) and were prepared by lyophilizing the given solute three times from 99.9% D_2O and redissolving in 0.5 mL of 99.99% D_2O. Where spectra in H_2O were required, the D_2O solutions were lyophilized and redissolved in 90% Milli-Q H_2O/10%D_2O.

Assignment of Free Hedamycin. NMR spectra of the free ligand were acquired at 400 MHz on a Varian VXR400 wide-bore spectrometer at 10 °C. Double quantum filtered (DQF) COSY, TOCSY, and ROESY experiments were performed using a 4000 Hz spectral width and 1024 data points in t_2 for 256 values of t_1 for the ROESY and TOCSY experiments and 512 values of t_1 for the DQF-COSY experiment. The ROESY and TOCSY data were acquired with a mixing time and spin lock time of 200 and 80 ms, respectively.

Analysis of the Hedamycin−d(CACGTG)$_2$ Adduct. Two-dimensional NMR experiments on $d(CACGTG)_2$ and on the hedamycin/$d(CACGTG)_2$ complex were performed at 10 °C on either a Bruker AMX500 (500 MHz) or AMX600 (600 MHz) spectrometer. DQF-COSY, TOCSY, and NOESY experiments were acquired with a spectral width of 5050.5 Hz at 500 MHz and 6098.6 Hz at 600 MHz. Four thousand ninety-six points were acquired in t_2 for each of 350 t_1 values for the DQF-COSY and TOCSY experiments and 512 t_1 values for the NOESY experiments. Presaturation of the HDO peak was achieved by placing the carrier frequency at the peak and applying low irradiation power (75dB) during the relaxation delay of 1.5 s. NOESY spectra were acquired using mixing times of 50, 150, and 300 ms. The TOCSY spectrum was acquired using a spin lock time of 80 ms.

^{1}H NMR spectra of exchangeable proton resonances were collected in 90%H_2O/10%D_2O, using 55 dB presaturation during the 1.5 s relaxation delay. Spectra of the free duplex were acquired at 2 °C, and spectra of the complex were acquired at 10 °C. NOESY spectra of the free and bound duplexes were acquired with a mixing time of 300 ms.

^{31}P NMR spectra were recorded on a Varian VXR400 wide-bore spectrometer at a frequency of 160 MHz. The phosphate signal from the buffer (pH 6.7) was used as the reference.

Computer Modeling. The crystal coordinates for hedamycin (Zehnder et al., 1979) were used as the starting point for modeling studies. The bond between C18 and the O of the epoxide ring was broken and replaced with an amino group to simulate a covalent attachment to the N7 of guanine. The atom potential types were redefined within the AMBER forcefield (Weiner et al., 1984, 1986) using Homans' extensions for the sugar rings (Homans, 1990) and the structure was energy minimized. Partial charges for the ligand were calculated using AM1 (Dewar et al., 1985) in the AMPAC/ MOPAC module of Insight and Discover (Biosym). A list of potential types and partial charges for hedamycin (and the modified guanine) used in calculations is available as Supporting Information. The DNA duplex $d(CACGTG)_2$ was built using the Biopolymer module of the Insight/Discover suite of programs, and the AMBER forcefield was selected.

The C18 of hedamycin was covalently connected to the N7 of G10. The N7 atom of the alkylated G10 was assigned planar sp^2 hybridization, and the chromophore was docked between the C3-G10 and G4-C9 base pairs by adjusting the torsion angles of the epoxide chain. Complexes were constructed with C18 in either an R or S configuration so that these could be compared. Molecular mechanics and dynamics calculations on the structures generated by the docking procedure were carried out using the Discover

program. Calculations were done using a 50% reduction of the 1−4 nonbonded interactions, as recommended in the InsightII/Discover program manual to compensate for the way in which the program manipulates the AMBER forcefield. A distance-dependent dielectric was employed to scale interatomic electrostatic interactions depending on the distance between the atoms (Warshel, 1979; Lavery et al., 1986). This procedure partially simulates the presence of solvent without causing dramatic increases in computational time and has been employed extensively in studies involving DNA (Lane et al., 1991; Kollman et al., 1981).

Distance restraints were employed in the molecular mechanics/dynamics calculations involving the use of an extra potential function in the forcefield and resulting in chosen pairs of atoms from the ligand and the DNA duplex being brought to within a fixed distance range. The atom pairs and distances used in this procedure were selected based on the observation of intermolecular NOEs. These were classed into broad categories of strong, medium, weak, and very weak, where the corresponding upper limits for each category were 2.5, 4.0, 5.0, and 6.0 Å. The NOE between the cytosine H5 and H6 protons was used as a reference (Reid et al., 1989), and the intensity of the NOE cross-peak was categorized based on build up rates determined from NOESY spectra acquired at different mixing times. The following protocol for molecular mechanics and simulated annealing was used: (i) after docking, the drug−DNA complex was minimized using a "steepest descents" gradient in order to remove energetic conflicts brought about by undue interatomic proximity; (ii) all NOE-derived distance restraints were applied simultaneously, and the complex was again minimized using molecular mechanics; (iii) the system was brought to equilibrium at a temperature of 300 K for 10 000 iterations prior to 4000 iterations of molecular dynamics; (iv) the simulated annealing was begun by reducing the temperature by 50 K before repeating the cycle of equilibration and molecular dynamics; (v) this was repeated until the temperature reached 0 K, when the drug−DNA complex was again energy minimized using molecular mechanics; and (vi) each of the last five steps was repeated 50 times, with the starting calculation vector being altered each time to search new areas of conformational space.

RESULTS

Assignment of DNA Duplex. The spectra of d(CACGTG)$_2$ proved to be typical for standard B-DNA, and assignment was carried out using established procedures (Gronenborn & Clore, 1985; Hosur et al., 1988; Wemmer, 1991). In contrast, the spectral characteristics of the adducted DNA duplex indicated that it was nonsymmetrical and differed considerably from standard B-DNA. For example, there are 12 distinct sugar spin systems distinguishable in the DQF-COSY spectrum of the complex, compared to six in the spectrum of the free duplex, indicating that the strands are no longer equivalent after the complex is formed. Consequently, the DNA duplex of the complex is numbered as shown in Figure 1.

The DQF-COSY spectrum allowed resonances arising from the sugar H1′, H2′, H2″, and H3′ protons to be identified and assigned to an individual spin system. The H4′ could only be partially assigned due to the absence of cross-peaks between A2H4′, G4H4′, and their corresponding H3′ protons. However, these correlations are observed in the TOCSY spectrum, thus allowing full assignment of the H4′ resonances. The H5′ and H5″ resonances were only partially assigned due to severe overlap of these resonances. A more extensive assignment of these protons relied on the analysis of NOESY spectra. The NOESY spectrum in D_2O was assigned based on the sequential patterns that arise due to the right-handed helical nature of B-DNA (Gronenborn & Clore, 1985). The fingerprint region of the complex is shown expanded in Figure 2. As the oligonucleotide strands in the duplex are not equivalent, sequential patterns can be observed for each strand. In the following discussion, NOEs are denoted as residue 1 atom name/residue 2 atom name.

Resonances from the cytosine H6 protons are the most straightforward to assign as they yield intense NOEs to cytosine H5 protons. Cytosine H6 resonances are located at 7.48, 7.53, 7.73, and 7.75 ppm. These assignments are also readily confirmed in the COSY spectrum, as no other aromatic resonances yield COSY cross-peaks. The cytosine H6 peaks at 7.73 and 7.75 ppm show only two NOEs in this region, one of which must be to the cytosine H5 and the other to H1′ from the sugar of the same residue. The absence of another NOE in this region suggests that these are the two terminal cytosines of the duplex, and, therefore, an NOE to protons on residues to the 5′ side cannot be present. These residues are numbered cytosine 1 and cytosine 7 arbitrarily.

An unbroken assignment pathway for strand 1 (residues 1−6) commences with C1H6/C1H1′ and can be traced through to the terminal G6H8/G6H1′, although the C3H1′/G4H8 NOE is extremely weak and is only observed at long mixing times. This allows sequence-specific assignment of both the aromatic resonances as well as the H1′ protons of strand 1. Strand 2 (residues 7−12) shows unbroken connectivities starting from G7H8/G7H1′ and ending with C9H6/C9H1′. The pattern begins again with T11H6/G10H1′ and continues through to G12H8/G12H1′. The missing C9H1′/G10H8 NOE is an interresidue NOE and potentially could be explained by an increase in the distance between these two protons. However, the intraresidue G10H1′/G10H8 NOE is also absent, which suggests that the G10H8 resonance is missing from this region of the spectrum. As is indicated below, this is consistent with alkylation.

NOEs between aromatic protons provide further confirmation of the aromatic assignments (Figure 2). In the NOE connectivity pattern for strand 1 there is a notable absence of an NOE between the C3H6 and G4H8, suggesting that the distance between these two residues is greater than that for other residues. Similarly, in strand 2 there is an absence of an NOE between C9H6 and G10H8. However, there is also an absence of NOEs between G10H8 and T11H6, indicating that the G10H8 resonance is not present in this part of the spectrum.

The sequential connectivity pattern formed by intranucleotide and internucleotide NOEs involving base H6,H8 and deoxyribose H2′,H2″ protons is traced for each strand in Figure 3. This provides further confirmation of the aromatic assignments as well as allowing assignment of the H2′/H2″ protons. Assignment of the H2′/H2″ protons was based on the intensities of the NOEs between H2′ and H2″ to the base H6,H8 protons at shorter mixing times (Wüthrich, 1986). In most residues, H2″ protons occur further downfield than H2′ protons; however, the opposite is true for the 3′-terminal guanine residues (G6 and G12) and the C3 residue. As-

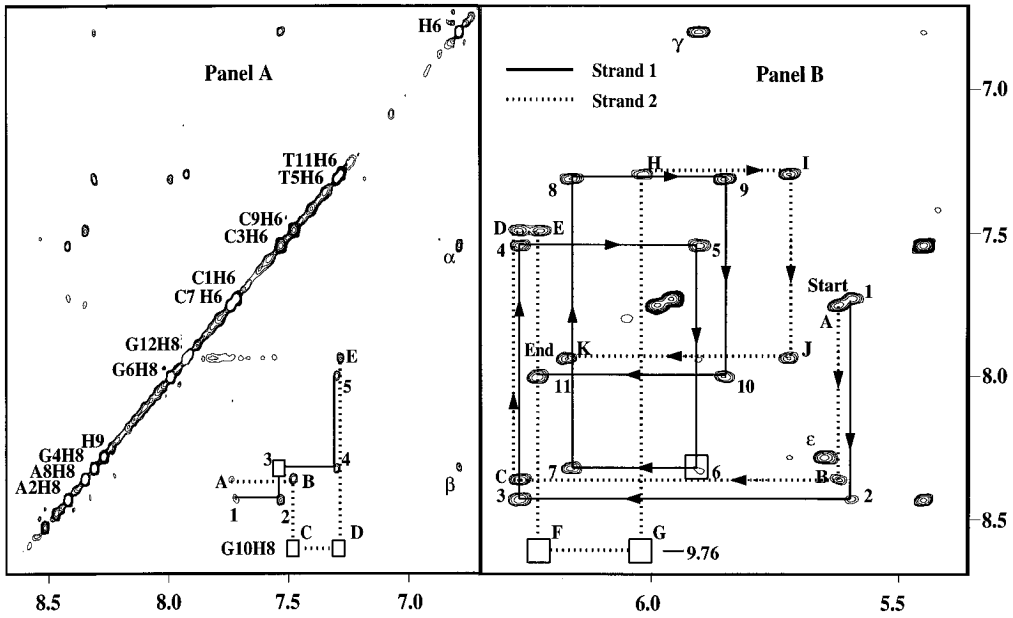

FIGURE 2: Expansion of the aromatic region (panel A) and the fingerprint region (panel B). In panel A the sequential NOEs between the stacked base pairs are numbered 1−5 for strand 1 and A−E for strand 2. The boxes mark the positions of the missing C3H6/G4H8 (3), C9H6/G10H8 (C), and G10H8/T11H6 (D) cross-peaks. Additional cross-peaks are labeled and assigned as C3H6/H6 (α) and G4H8/H6 (*β*). In panel B the intranucleotide and internucleotide NOEs involving base H6,H8 and deoxyribose H1′ protons form the characteristic sequential pattern for B-DNA as follows: C1H6/C1H1′ → A2H8/C1H1′ → A2H8/A2H1′ → ... → G6H8/T5H1′ → G6H8/G6H1′. The sequential NOEs are numbered 1−11 for strand 1 and A−K for strand 2. The boxes indicate breaks in the sequential pattern caused by the missing NOEs G4H8/C3H1′ (6), G10H8/C9H1′ (F), and G10H8/G10H1′ (G). The additional labeled cross-peak is assigned as H6/C3H1′ (*γ*).

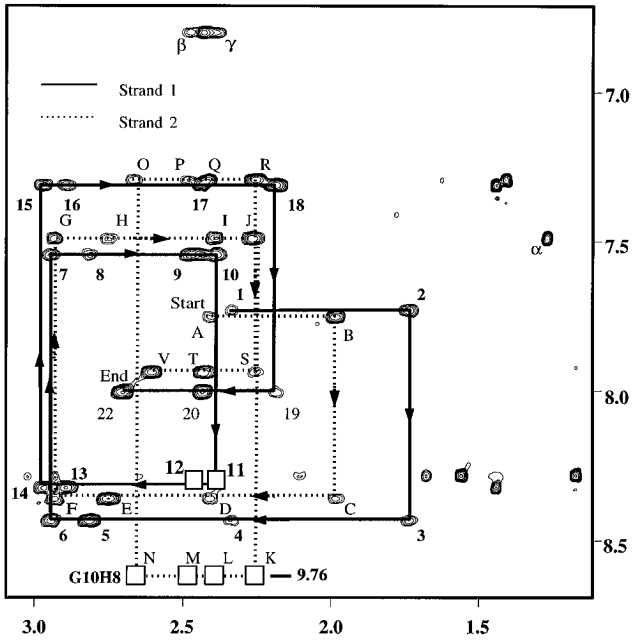

FIGURE 3: Intranucleotide and internucleotide NOEs involving base H6,H8 and deoxyribose H2′,H2″ protons make up a sequential pattern from C1H6/C1H2′,H2″ → A2H8/C1H2′,H2″ → A2H8/A2H2′,H2″ → ... → T5H6/T5H2′,H2″ → G6H8/T5H2′,H2″ → G6H8/G6H2′,H2″. The sequential NOEs of strand 1 are numbered 1−22 and those of strand 2 are labeled A−V. Breaks in the sequential pattern are indicated by boxes and are due to the absence of the NOEs G4H8/C3H2′,H2″ (11 and 12) in strand 1 and G10H8/C9H2′,H2″ (K and L) and G10H8/G10H2′,H2″ (M and N) in strand 2. Note that NOEs 20 and 21 are overlapped, as are NOEs T and U.

signments of the H2′,H2″ resonances were confirmed by the greater intensity of H1′−H2″ compared to H1′−H2′ NOEs at shorter mixing times (Baleja et al., 1990).

The sequential connectivity for strand 1 begins with C1H6/C1H2′,H2″ and continues unbroken through to C3H6/C3H2′,H2″. The interresidue G4H8/C3H2′,H2″ contacts are missing from the spectrum, and a very weak NOE between these two residues appears only at longer mixing times (300 ms). The sequential connectivity continues from G4H6/G4H2′,H2″ cross-peaks through to G6H6/G6H2′,H2″. Sequential assignments can also be made for strand 2 beginning with the C7H6/C7H2′,H2″ cross-peaks. The interresidue G10H8/C9H2′,H2″ and the intraresidue G10H8/G10H2′,-H2" NOEs are, however, missing from the spectrum. These breaks in the sequential connectivities provide evidence that the distance between the C3 and G4 residues is greater than for other base pairs and that the G10H8 resonance is not present in this region of the spectrum. Further confirmation for the absence of G10H8 is provided by NOEs between the thymine methyl protons and aromatic protons. Interresidue NOEs between thymine methyls and aromatic base protons of the preceding residue are expected in B-DNA. A cross-peak between T5CH3 and G4H8 was observed; however, no such cross-peak was observed between T11CH3 and the aromatic region.

Intraresidue NOEs between the assigned H1′ protons and the H3′, H4′, H5′, and H5″ protons allowed sequence-specific assignments to be extended through the sugar spin systems. Eleven H1′−H3′ NOEs are observed, with the missing one being the T11H1′−H3′ NOE, probably due to the T11H3′ resonance being overlapped with the water resonance. NOEs between H3′ and H4′ were assigned despite overlap with other NOEs in some regions. The assignment of these NOEs was aided by correlation with longer range NOEs observed between H4′ and H1′ protons at longer mixing times. In some cases NOEs are also observed between H4′ protons and aromatic protons at longer mixing times. These NOEs confirm the assignments of H4′ protons made from scalar

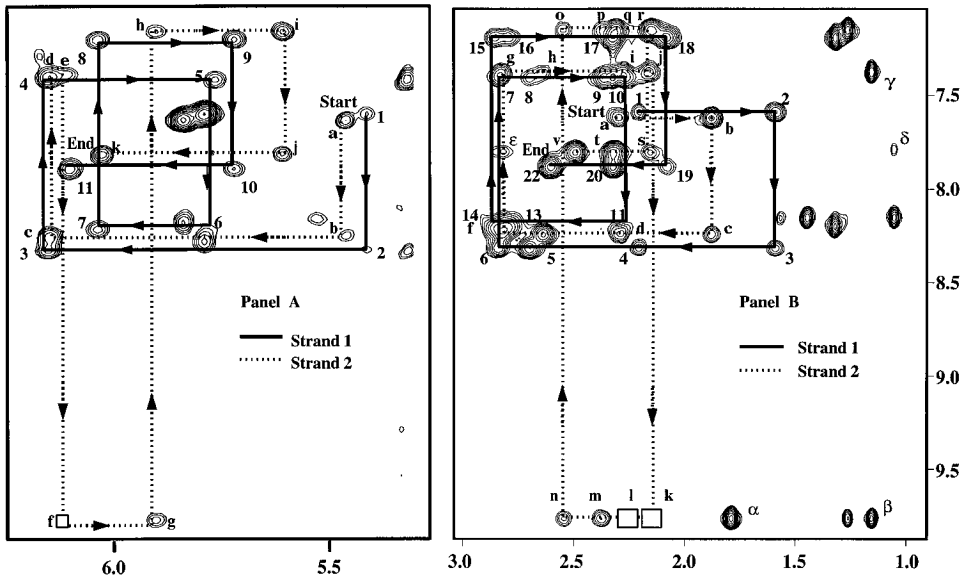

FIGURE 4: Fingerprint region (panel A) and H6,H8−H2′,H2″ region (panel B) of the NOESY spectrum (300 ms) acquired in 10% D_2O/90% H_2O. The sequential patterns are the same as those shown in Figures 2 and 3. The intranucleotide NOEs G10H8/G10H1′ (g) in panel A, G10H8/G10H2′ (m), and G10H8/G10H2″ (n) in panel B that were absent in the D2O spectra are now observed due to the appearance of the G10H8 resonance at 9.76 ppm. The boxes mark the absence of the internucleotide NOEs G10H8/C9H1′ (f) in panel A, G10H8/C9H2′ (k), and G10H8/C9H2″ (l) in panel B. The additional labeled NOEs are assigned as G10H8/$CH_3$19 (α), G10H8/$CH_3$15 (β), C9H6/$CH_3$15 (γ), A8H2/$CH_3$8″ (δ), and A2H2/N-CH_3′ (ϵ).

couplings and allow their sequence-specific assignment.

NOEs between H5′/H5″ protons and H1′ protons, as well as to H3′ and aromatic protons, are observed at longer mixing times. These contacts allow assignment of most H5′/H5″ protons despite overlap in some regions. Two notable exceptions are the C3H5′ and C9H5′, protons which could not be assigned either due to an absence of cross-peaks in some regions or overlap in others. However, the observation of two very weak cross-peaks in the COSY spectrum suggests that these resonances are overlapped with H3′ resonances at 4.28 and 4.20 ppm.

Exchangeable Resonances. Exchangeable resonances are observed in the 1D spectrum of the complex in H_2O between approximately 6.4 and 14.1 ppm. All of these resonances are less intense and broader than the nonexchangeable resonances except for a single sharp peak at 9.76 ppm. This signal is of particular interest as it shows NOEs to the G10H1′ as well as to G10H2′,H2″ protons. Consequently it is assigned as the G10H8 resonance, which is absent in the spectrum acquired in D_2O. Other NOEs expected for this resonance are also observed, including contacts with T11H6 and T11CH_3, thus confirming this assignment. With the appearance of this resonance and of the intraresidue NOEs to the deoxyribose ring, the sequential connectivity patterns of strand 2 are more complete compared to those measured in D_2O. However, there is still an absence of interresidue NOEs between residues C9 and G10 (Figure 4), suggesting that the distance between these bases has increased.

The exchangeable DNA resonances were assigned on the basis of the NOEs to adjacent base pairs. The resonance with the greatest chemical shift (14.08 ppm) shows a large number of NOE contacts, some of which are to resonances from the ligand. A number of other NOEs are to resonances from the G10 and C9 residues, and, consequently, this resonance was assigned to the T5 and T11 hydrogen-bonded imino protons. Two other resonances in the hydrogen bonded imino region of the spectrum (at 13.58 and 11.87 ppm) show NOEs to A8H2 and A2H2, respectively, and were assigned to G4 and G10 NH protons, respectively. The G4 NH proton shows an NOE to the T5CH_3, which is consistent with this assignment. The G10NH proton also shows NOEs to two other exchangeable resonances at 6.47 and 7.25 ppm, and these were assigned as the G10NH_2 protons.

The C1 and C7 NH_2 protons were easily identified from NOEs to their respective H5 protons. NOEs are also observed between the hydrogen bonded and non-hydrogen-bonded proton of each amino proton pair. Two pairs of exchangeable resonances also appeared at 6.46 and 7.75 ppm, and at 6.91 and 7.30 ppm, which show no other NOEs except within the pairs. These resonances were assigned as the C3 and C9 NH_2 protons; however, it is not possible to distinguish which pair is which. B-DNA is expected to show NOEs between cytosine NH_2 and H5 protons. The lack of expected NOEs to the C3 and C9H5 resonances may be due to structural distortions because of intercalation of the ligand or to effects of presaturation as these H5 resonances are close to the water resonance. A tabulation of the resonance assignments for the d$(CACGTG)_2$ and hedamycin−d$(CACGTG)_2$ duplexes is available as Supporting Information.

Ligand Assignments. The free hedamycin resonances in D_2O at 10 °C were assigned using a combination of DQF-COSY, TOCSY, ROESY, and NOESY spectra. The same procedure was used to assign the ligand resonances of the complex. This involved identifying the spin systems for the epoxide side chain and the two sugar residues (Figure 1) in DQF-COSY and TOCSY spectra. Cross-peaks arising from the three major spin systems of hedamycin were readily distinguishable following elimination of cross-peaks belonging to the 12 deoxyribose spin systems. The most distinguishable in the DQF-COSY spectrum is the ring E spin system. This shows an unbroken connectivity pattern beginning at the H6′ resonance (5.64 ppm), located downfield of other sugar ring resonances, and continues through to the $CH_3$7′ resonance (1.68 ppm).

Ring F does not have such an extensive spin system, as the C4″ carbon is substituted with a methyl group. The C6″−C5″ and the C3″−C2″−C7″ portions of the sugar ring can therefore be thought of as separate spin systems. There is a resonance (5.65 ppm) almost overlapped with the H6′ resonance (5.64 ppm) which displays DQF-COSY and TOCSY cross-peaks to two other resonances further upfield at 3.22 and 2.65 ppm. These resonances were assigned as the H6″, H5a″, and H5b″ protons, respectively. The methyl resonance at 1.57 ppm shows only one DQF-COSY and TOCSY cross-peak to a resonance at 4.31 ppm and had no further connectivity. These resonances were assigned as $CH_3$7″ and H2″. The connectivity to H3″ is difficult to observe in the TOCSY or DQF-COSY spectrum, as this region of the spectrum is overlapped with deoxyribose resonances. Resonances arising from the dimethylamino groups of both sugars and the $CH_3$8″ of ring F could not be assigned from the TOCSY and DQF-COSY spectra due to the absence of scalar coupling to these substituents. Assignment of these groups was dependent on the observation of intramolecular NOEs (see below).

The unbroken connectivity from $CH_3$19 (1.92 ppm) to H16 (3.52 ppm) of the epoxide side chain is easily distinguished in both the TOCSY and DQF-COSY spectra. This allows all the protons of the side chain to be unambiguously assigned, except for $CH_3$15, which is isolated from the ^{1}H spins of the rest of the chain. Assignment of this resonance is dependent on the NOESY spectra. The methyl resonance at 1.27 ppm shows NOEs to H16, H17, H18, and $CH_3$19, which led to the assignment of this resonance as $CH_3$15.

The NOESY spectra confirm the assignments made from the DQF-COSY and TOCSY spectra and were also used to assign the dimethylamino and $CH_3$8″ groups of the sugar rings. It is evident that the dimethylamino groups are overlapped in the region between 2.9 and 3.1 ppm. Two NOEs between the easily distinguishable H5a″ resonance (3.22 ppm), and peaks in this region clearly mark the position of the ring F dimethylamino resonances at 2.93 and 3.02 ppm. Similarly, the ring E dimethylamino resonances at 2.90 and 2.97 ppm were assigned based on NOEs between the H5a′ and H5b′ protons of ring E and the dimethylamino region. The methyl resonance furthest upfield in the spectrum (1.18 ppm) shows a number of NOEs to ring F resonances including H6″, H2″, H5a″, and H5b″. Consequently, this was assigned as the $CH_3$8″ resonance. The ^{1}H resonances of the chromophore were assigned from NOESY and TOCSY spectra. The aromatic resonance at 8.27 ppm shows NOEs to resonances from both sugar rings E and F (e.g., H6′, H2′, H3′, $CH_3$7′, H2″, $CH_3$7″, $CH_3$8″). It also shows a very weak TOCSY cross-peak to the H6′ resonance at 5.64 ppm and was therefore assigned as H9. The resonance at 6.79 ppm shows an NOE to a methyl resonance at 2.44 ppm as well as to a number of established DNA resonances. This NOE also corresponds to a very weak TOCSY cross-peak, and, consequently, these resonances were assigned as H6 and $CH_3$13, respectively.

The assignment of the vinylic H3 proton of ring A was made difficult by the fact that no scalar coupling was expected for this proton and the only possibility for dipolar coupling was from the $CH_3$15 of the epoxide, depending on the orientation of the epoxide chain. The $CH_3$15 proton shows NOEs to two protons that resonate at 6.23 and 7.48 ppm and are likely candidates for the hedamycin H3 resonance. The most downfield of these two resonances was earlier assigned unambiguously as C9H6, and since this resonance is clearly not overlapped with any other resonances, it was ruled out as a possibility. The other NOE is to an overlapped region of the spectrum which contains the C9, G6, A2, and A8 H1′ protons. It is likely that the H3 proton of ring A is also overlapped with these resonances (6.23 ppm). Assignments of the free and bound hedamycin resonances are available as Supporting Information.

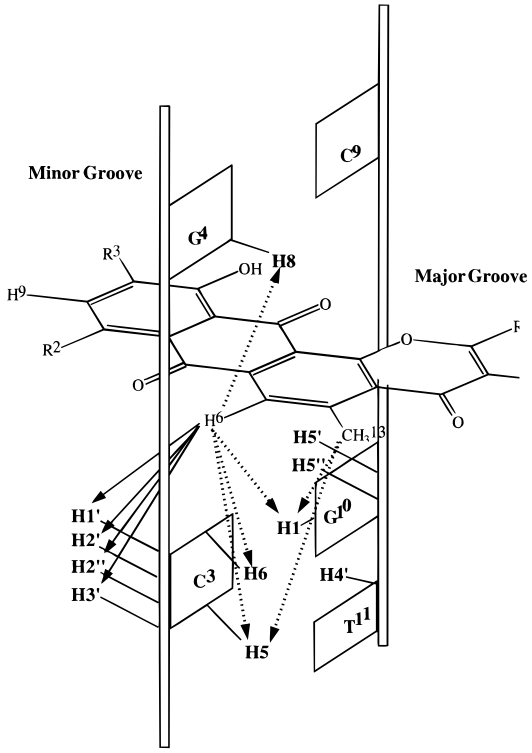

FIGURE 5: Schematic representation of NOEs observed to the chromophore of the ligand. Contacts to major groove protons are shown as dotted arrows and contacts to the minor groove are shown as full arrows. The H9 proton of the chromophore makes contact with G10H5′, G10H5″, and T11H4′; however, these are not shown for the purpose of clarity.

Intermolecular NOEs. The assignment of d(CACGTG)$_2$ and hedamycin resonances of the complex allowed the identification of a total of 61 intermolecular NOEs between hedamycin and DNA, including contacts to protons located on the chromophore, the epoxide chain and the sugar groups (table of NOEs available as Supporting Information). These allow the orientation of the ligand within the binding site to be defined. Protons located on the chromophore make NOE contacts with a number of protons on the C3 and G4 residues that are located in both the major and minor grooves (Figure 5). NOEs to the epoxide chain are observed from residues C9, G10, and T11 and all involve contacts to protons located in the major groove, with the exception of the two very weak NOEs observed between C9H1′, G10H1′ and hedamycin $CH_3$15. The sugar groups of the ligand exhibit NOEs exclusively to protons located in the minor groove (Figure 6). The E ring makes contact predominantly with residues from the nonalkylated strand (strand 1), including G4, C3, and weaker contacts to A2 and T5 residue, although NOEs are also observed between the N-methyl protons and the deoxyribose ring of T11 (Table 1, Supporting Information). The F-ring only makes contact to the alkylated strand (strand

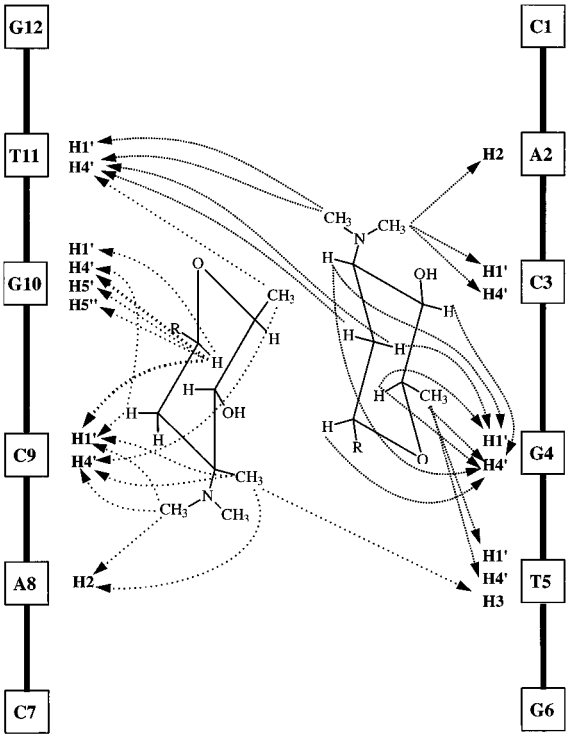

FIGURE 6: Schematic representation of ring E (shown on the right) and ring F (shown on the left) within the minor groove of the duplex. Intermolecular NOE contacts from each ring to the DNA duplex are indicated by arrows.

2), with NOEs being observed to residues C9 and G10 and weaker contacts to A8 and T11.

DISCUSSION

Alkylation of the N7 of Guanine. From the results of our DNA sequencing studies (Murray et al., 1995; Prakash et al., 1995), it was anticipated that hedamycin would alkylate the central guanine of the d(CACGTG)$_2$ sequence via one of the two epoxide groups. The spectrum acquired in H_2O shows a resonance at 9.76 ppm which was subsequently assigned as G10H8, based on observed NOEs to G10H1′, G10H2′, and G10H2″. This resonance is absent in spectra acquired in D_2O. Inspection of the NOESY spectrum acquired in D_2O reveals that expected intraresidue NOEs to the G10H8 resonance (e.g., G10H8/G10H1′, G10H8/G10H2′,-H2″) are missing, confirming that the peak has not merely shifted but has disappeared from the spectrum (Figures 2, 3, and 4). The lability of this proton and the deshielding compared with the free guanine H8 resonance are consistent with covalent attachment of the ligand to the N7 of G10 (Gopalakrishnan et al., 1989, 1990, 1992). The resulting positive charge on the guanine was found to cause a dramatic increase in the acidity of its H8 proton and therefore the disappearance of its ^{1}H NMR signal in D_2O. In H_2O, the H8 proton of the quaternized purine was found to be deshielded by approximately 2 ppm relative to that of the free DNA.

Hedamycin contains two epoxide groups, with the most likely candidates for covalent attachment along the epoxide chain being C16, C17, and C18. The largest chemical shift perturbation in the adduct was for H18, which was deshielded by approximately 2 ppm. A shift of this magnitude indicates that C18 of hedamycin is the epoxide carbon involved in purine alkylation. By contrast, H16 and H17 underwent shifts of less than 0.5 ppm upon adduct formation. The NOEs observed between the hydrogens of the epoxide-containing side chain and those of the major groove also support this as the alkylating moiety (Figure 7).

Intercalation of the Adducted Hedamycin. ^{31}P NMR spectra of the free duplex and 1:1 hedamycin−DNA covalent complex were acquired to obtain evidence for helix unwinding (Patel, 1974, 1976; Scott, et al., 1988; Gao, & Patel, 1988; Searle, et al., 1988). The ^{31}P resonances of the free duplex are overlapped in the region −3.6 to −4.0 ppm. However, in the spectrum of the 1:1 complex, two distinct signals appear at −2.13 and −3.09 ppm. The deshielding of at least two ^{31}P nuclei is characteristic of unwinding of the helix due to an intercalative mode of binding (Gorenstein & Lai, 1989, and references therein; Searle, 1993).

The intercalation site is revealed by NOESY experiments. In spectra acquired in D_2O, there is an absence of interresidue NOEs between residues C3 and G4 of strand 1 (e.g., C3H6/G4H8, C3H1′/G4H8, G4H8/C3H2′,H2″) (Figures 2 and 3). The spectrum acquired in H_2O, in which the G10H8 resonance is observable, confirms that there is a similar absence of interresidue NOEs between residues C9 and G10 of strand 2 (e.g., G10H8/C9H1′, G10H8/C9H2′,H2″) (Figure 4). These breaks in the sequential connectivity are consistent with intercalation of the chromophore between the base pairs

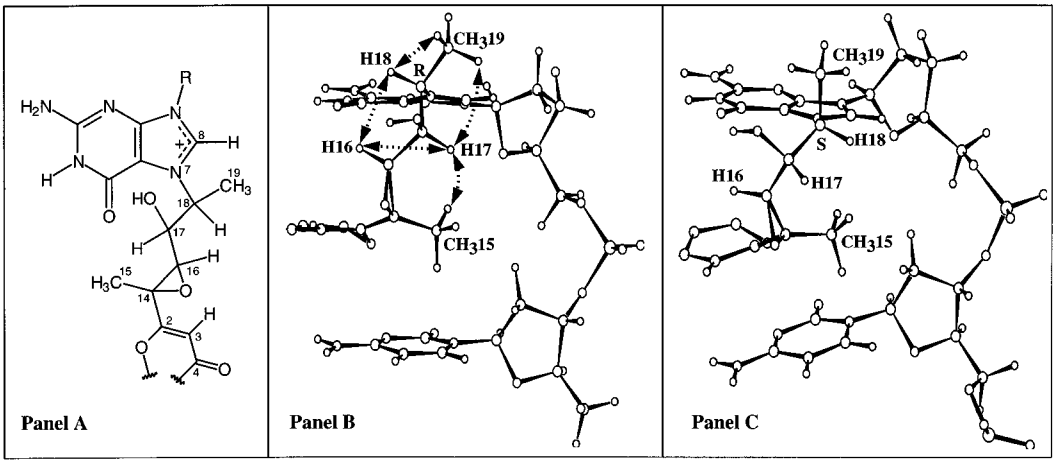

FIGURE 7: Chemical structures of the epoxide chain and guanine residue following alkylation are shown in panel A. Panels B and C show the structure calculated when the configuration of the C18 atom is R and S, respectively. NOEs that were observed in the 50 ms NOESY are indicated by arrows in panel B.

C3-G10 and G4-C9 (Searle & Bicknell, 1992; Zhang & Patel, 1990).

Orientation within the Binding Site. NOEs to the chromophore include contacts between the H6 proton, which is located on ring B of the chromophore, and protons on the C3 and G4 residues located in both the minor groove and the major groove (Figure 5). NOEs are also observed between H6, $CH_3$13 of ring B, and the G10NH1 proton that is not exposed to either groove (Figure 5). These contacts are consistent with intercalation of the chromophore between the base pairs C3-G10 and G4-C9 so that ring B is stacked between the bases of these residues, in a position where the major groove protons as well as minor groove protons are within 5 Å of H6. The NOEs between hedamycin H6 and other protons of the C3 sugar moiety indicate that this edge of the chromophore, which is opposite to that bearing the epoxide chain and ring F, is closer to strand 1 of the DNA duplex. The NOE contact to the hedamycin $CH_3$13 from the C3H5 proton and the lack of any NOEs to the minor groove establishes that the end of the molecule comprising rings A and B protrudes into the major groove.

The NOEs between G10H5′,H5″, T11H4′, and hedamycin H9 indicate that ring D is situated in the minor groove and suggest that ring D is closer to strand 2 (i.e., the alkylated strand) of the duplex than to strand 1. As ring B of the chromophore has been shown to contact strand 1, this implies that the long axis of the intercalating ligand is not perpendicular to the long axis of the flanking base pairs but is at an angle to the long axis of the C3−G10 base pair.

NOEs observed between the epoxide chain and the DNA duplex firmly establish that the epoxide chain is located in the major groove, consistent with alkylation of the N7 of residue G10. The NOEs that best define the position of the epoxide chain are the contacts between the C9 residue and hedamycin $CH_3$15, together with NOEs between hedamycin $CH_3$19, H18, and T11CH_3. These show that the epoxide chain spans a region of space between the C9 (G10) and T11 residues and further suggest that the second epoxide group in the chain (C17, C18) is well placed to form a covalent bond to the N7 of G10. The G10H8 proton shows a strong NOE to $CH_3$19 and a weaker NOE to $CH_3$15, further suggesting that C18 is better placed to form a covalent bond with G10N7.

The placement of ring D in the minor groove is corroborated by NOE contacts of the sugar groups to protons located exclusively in the minor groove. The contacts from ring E to the nonalkylated strand and from ring F to the alkylated strand are consistent with the orientation of the chromophore described above. Ring E is located on the opposite side of the chromophore to the alkylating epoxide chain (i.e., the same side as H6) and should therefore be located closer to the non-alkylated strand. NOEs observed between DNA and the N-$(CH_3)_2$ and $CH_3$7′,$CH_3$7″ (Figure 6) of the sugar rings in hedamycin help to best define the orientation of the sugar rings within the minor groove. The N-$(CH_3)_2$ of ring E makes a weak contact with A2H2 which is located on the floor of the minor groove as well as medium intensity NOE contacts to H1′ and H4′ protons from residues C3 and T11. This clearly places the 4″ end of the ring toward the C1-G12 end of the intercalation site. Contact between the N-$(CH_3)_2$ protons and protons located on opposite strands is possible because the helical nature of the strands causes the deoxyribose rings of these residues to be located so that they face each other across the minor groove. The NOEs are thus consistent with the bulky methyl groups making contact with protons on opposing walls of the minor groove. Consistent with this proposed orientation of ring E are the NOEs between T5H1′, T5H4′, and $CH_3$7″. The majority of the ring E protons make contact with the H1′ and H4′ protons of G4 suggesting that the plane of the ring lies close to the plane of the minor groove wall made up by the backbone of the nonalkylated strand. NOEs are observed from the ring E H5′ protons to T11 of strand 2; however, these are extremely weak and are still consistent with placement of this ring close to strand 1.

Similarly, the N-$(CH_3)_2$″ and $CH_3$8″ of ring F show weak NOE cross-peaks to A8H2 as well as to T5H3, which are both located on the floor and toward the center of the minor groove. These contacts suggest that ring F is oriented toward the G6-C7 end of the duplex. The large number of NOEs observed to the C9 and G10 residues and the lack of NOEs to strand 1 indicates that ring F is close to the alkylated strand. The NOE between $CH_3$7″ and T11H4″ confirms that the orientation of this ring is toward the G6-C7 end of the duplex.

Computational Refinement of the Model. The qualitative model deduced from the NMR data was refined using computational methods described in Materials and Methods. This model of the three-dimensional structure of hedamycin bound to the hexanucleotide duplex in solution involves the anthrapyran chromophore intercalated between the 5′-CG-3′ base pairs and threading the helix with the two sugar rings (rings E and F in Figure 1) placed in the minor groove and the bisepoxide side chain in the major groove. The long axis of the chromophore is not orthogonal to the long axis of the flanking base pairs but, instead, is oriented with the major groove end of the chromophore closer to the nonalkylated strand and the minor groove end closer to the alkylated strand (Figure 8).

The model suggests that the intercalation site is slightly wedge shaped. Evidence to support such a conformation is present in the fingerprint region of the NOESY spectrum in that a low intensity NOE is observed between C3H6 and G4H1′, whereas no such interresidue NOE is observed between C9H6 and G10H1′ of the alkylated strand. This distortion of the helix is analogous to that observed for nogalamycin, where the wedge shaped binding site was due to the chromophore being located closer to one strand than the other (Searle et al., 1988; Zhang & Patel, 1990). However, in this case the chromophore occupies a more central position between the two strands. Strain in the epoxide chain of the covalently bound ligand appears to be the cause of an increased distance between C9 and G10 relative to C3 and G4 (Figure 8).

The terminal epoxide carbon of the bisepoxide side chain, C18, is covalently attached to the N7 atom of guanine, which is to the 3′ side of the intercalated chromophore. The epoxide chain was modeled with C18 bonded to G10 N7 in both an R and S configuration (Figure 7). From an analysis of the atomic distances measured in these models and based on NOEs observed in the 50 ms NOESY spectrum, the R configuration appears to be more likely. At this short mixing time, an NOE is observed between H18 and H16, but not between H18 and H17. While the R configuration places H18 closer to H16, H18 and H17, being in an *anti* arrangement, are significantly further apart. In the S

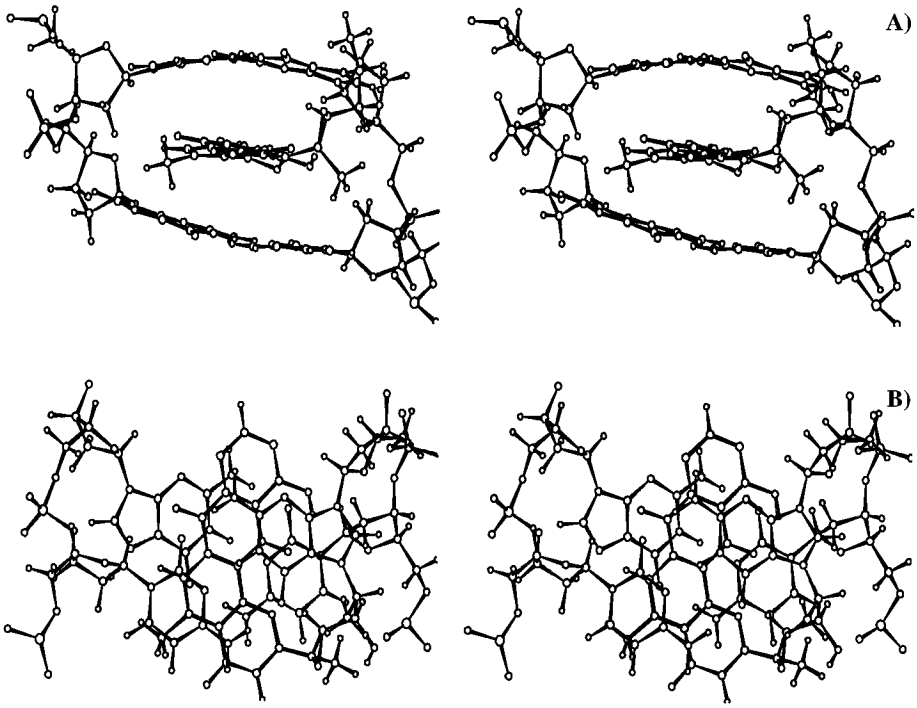

FIGURE 8: Two stereoviews of the intercalation site: (A) highlights the wedge-shaped binding site; and (B) the structure is rotated forward by 90° to highlight the orientation of the chromophore in relation to the flanking base pairs.

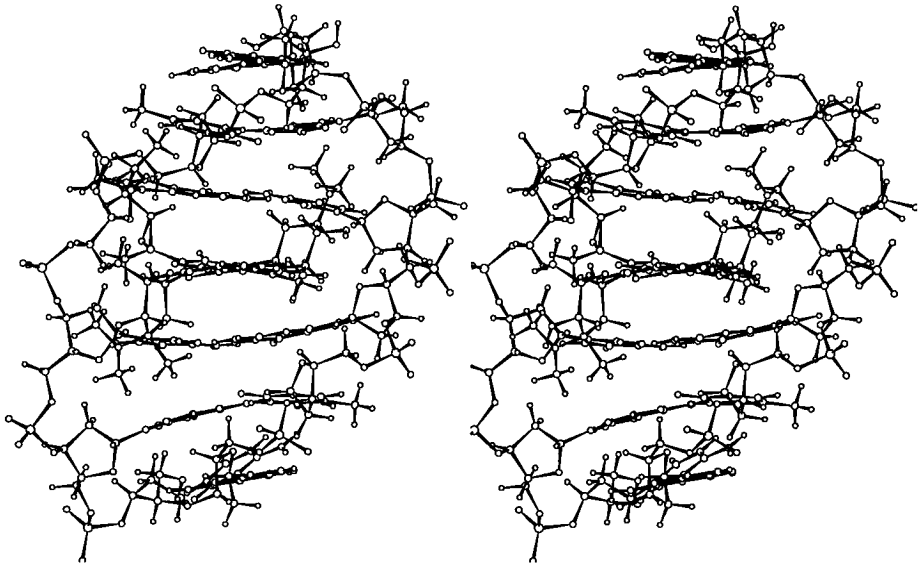

FIGURE 9: Stereoview looking into the minor groove that highlights the orientation of the hedamycin sugar groups (rings E and F).

configuration, the opposite situation would occur. That is, H18 and H17 would be in a *syn* arrangement, and thus a strong NOE would be expected, while H16 and H18 would be separated by a large distance making the observation of an NOE unlikely. NOEs observed between H17 and CH_3-15, and H17 and $CH_3$19, are also consistent with an R configuration. These NOEs are of approximately the same intensity, suggesting that the distance between H17 and CH_3-15 is similar to the distance between H17 and $CH_3$19. This is the case in the R configuration, whereas the S configuration results in a greater distance between H17 and $CH_3$19.

The angolosamine and *N*,*N*-dimethylvancosamine sugar rings are both located in the minor groove and show some variation in conformation compared to the crystal structure of free hedamycin. The torsion angles between ring E and ring F and the chromophore (i.e., C9-C8-C6′-C5′ and C9-C10-C6″-C5″) were found to be $-100.0° \pm 3°$ and $86° \pm 2°$ compared with 74.2° and −104.2°, respectively, in the crystal structure. This represents a significant degree of rotation given the bulky nature of the rings; however, the result is that ring E is placed toward the 3′ side of the alkylation site and ring F is toward the 5′ side of the alkylation site (Figure 9). This results in a complementarity between the sugar groups and the minor groove that allows the narrow minor groove to accommodate both rings. In addition, van der Waals interactions between the rings and the minor groove walls are maximized. Each ring is positioned so that the plane of the ring lies approximately parallel with the plane of the minor groove wall. Ring E is predominantly associated with the nonalkylated strand, making significant van der Waals contacts with residues C3 and G4. Ring F, on the other hand, is more closely associated with the alkylated strand and makes van der Waals contact with residue C9.

In this model, the nitrogens of each N-$(CH_3)_2$ group are in close proximity to the O2 atoms of the C3 and C9 residues. This suggests that there is the possibility of hydrogen bonding between the charged dimethylamino group and the C3 and C9 bases in the minor groove. The orientation of the N-methyl groups, however, needs to be better defined to confirm this.

Sequence Specificity and Comparison with other Ligand−DNA Complexes. The models for the interaction of altromycin B and hedamycin with DNA suggest that the sugar substituents at the C5, C8, and C10 positions influence the covalent interaction by serving to guide the reacting epoxide moiety to the alkylation site (i.e., N7 of guanine). In the case of altromycin B, the C5 sugar and the disaccharide at the C10 position act to place the chromophore at a position perpendicular to that of the flanking base pairs, which causes the reactive epoxide group on the four carbon C2 side chain to be brought closer to the alkylation site (Hansen & Hurley, 1995). Hedamycin contains a longer six carbon C2 side chain and two epoxide groups, and our results, in agreement with those of Hansen et al. (1995), show that it is the epoxide group farthest from ring A that reacts. The placement of the C8 and C10 sugars of hedamycin in the minor groove results in the chromophore being at more of an angle to the flanking base pairs (Figure 8). Thus, in the models of hedamycin binding to 5′-CG and 5′-TG, the positioning of ring A toward the non alkylated strand in the major groove allows the longer side chain to be better accommodated and positions the second epoxide group for nucleophilic attack by N7 of guanine. Our results also suggest that there is some steric strain caused by the alkylation, and this would be magnified if ring A were positioned closer to that alkylated strand. This is discussed further below.

The model of hedamycin interacting with 5′-CG-3′ indicates that there is a higher degree of complementarity between the walls and floor of the minor groove and the orientation of the sugar groups compared with hedamycin binding to 5′-TG. The sugar groups of hedamycin are placed to the side of the exocyclic amine group of each GC base pair so that they are wedged between the amino groups and the walls of the minor groove. This causes the sugar groups to be parallel with the walls of the minor groove and explains the large number of NOE contacts between ring F and the alkylated strand and ring E and the nonalkylated strand. In addition, this arrangement accounts for the small number and extremely low intensity of NOEs between each of these rings and the opposite wall of the minor groove. The effect of the exocyclic amine group of guanine on the angolosamine ring is also seen in the hedamycin−5′-TG-3′ model (Hansen et al., 1995). The absence of this amino group in the TA base pair to the 5′ side of the alkylated guanine allows ring F to be more parallel with the floor of the groove, thus decreasing the extent of van der Waals interactions with the minor groove wall and reducing the complementarity. The preference for 5′-CG-3′ over 5′-TG-3′ sequences suggests that this complementarity is a determining factor in the sequence selectivity of hedamycin. The placement of a guanine to the 5′ side of the alkylated guanine would result in a great deal of steric hindrance between the exocyclic amine and ring F, as the amine group in this case would be located closer to the alkylated strand. Similarly, this model suggests that the presence of a 5′ adenine also decreases complementarity compared with the presence of a 5′ pyrimidine.

The influence of the van der Waals contact between the sugar groups and the minor groove does not extend to a significant degree beyond the two base pairs between which the ligand intercalates and therefore does not have any influence on the requirement for a thymine residue to the 3′ side of the alkylated guanine. In the major groove, however, there is a strong NOE contact between the terminal methyl group of the epoxide and the T11CH_3 located on the 3′ side of the alkylated guanine. The preference for this thymine could thus be due to a hydrophobic interaction between the terminal $CH_3$19 of the epoxide chain and the thymine residue on the 3′ side of the alkylated guanine. The model shows that, particularly with C18 in an R configuration, there is a hydrophobic cluster formed between one edge of the epoxide chain and the edge of the major groove. From the epoxide chain this includes the $CH_3$15, which is turned in toward the floor of the groove rather than exposed to solvent in the major groove cavity, H17, and $CH_3$19. From the DNA duplex, the cluster includes G10H8, G10H2′, and G10H2″ and is "capped" by the T11CH_3. As for the interaction of the sugar groups with the minor groove, this hydrophobic cluster has the potential to favor alkylation at 5′-CGT-3′ by serving to guide the C18 atom of the epoxide chain toward the N7 alkylation site. Our studies indicate that there is some strain present in the covalently bound C2 side chain of hedamycin, which suggests that the chain could extend beyond the plane of the G10 base. Thus, the hydrophobic interaction, and in particular the interaction with the T11CH_3, serves to limit this extension and therefore better position the epoxide for reaction.

SUPPORTING INFORMATION AVAILABLE

Six tables listing assignments of the nonexchangeable and exchangeable ^{1}H DNA resonances of the free and bound d$(CACGTG)_2$ duplex, assignments of free and bound hedamycin ^{1}H resonances, intermolecular NOEs, and AMBER potential types and partial charges of hedamycin and the adducted guanine used in molecular modeling (6 pages). Ordering information is given on any current masthead page.

REFERENCES

Baleja, J. D., Germann, M. W., Van de Sande, J. H., & Sykes, B. D. (1990) *J. Mol. Biol. 215*, 411−428.
Dewar, M. J. S., Zoebisch, E. G., Healy, E. F., & Stewart, J. J. P. (1985) *J. Am. Chem. Soc. 107*, 3902−3909.
Gao, X., & Patel, D. J. (1988) *Biochemistry 27*, 4340−4349.
Gopalakrishnan, S., Stone, M. P., & Harris, T. M. (1989) *J. Am. Chem. Soc. 111*, 7232−7239.
Gopalakrishnan, S., Harris, T. M., & Stone, M. P. (1990) *Biochemistry 29*, 10438−10448.
Gopalakrishnan, S., Xiucai Liu, & Patel, D. J. (1992) *Biochemistry 31*, 10790−10801.
Gorenstein, D. G. (1984) in *Phosphorus-31 NMR. Principles and Applications* (Gorenstein, D. G., Ed.) Academic Press, New York.
Gorenstein, D. G., & Lai, K. (1989) *Biochemistry 28*, 2804−2812.
Gronenborn, A. M., & Clore, G. M. (1985) *Prog. Nucl. Magn. Reson. Spectrosc. 17*, 1−32.
Hansen, M., & Hurley, L. (1995) *J. Am. Chem. Soc. 117*, 2421−2429.
Hansen, M., Yun, S., & Hurley, L. (1995) *Chem. Biol. 2*, 229−240.
Homans, S. W. (1990) *Biochemistry 29*, 9110−9118.
Hosur, R. V., Govil, G., & Miles, T. H. (1988) *Magn. Reson. Chem. 26*, 927−944.

Kollman, P. A., Weiner, P. K., & Dearing, A. (1981) *Biopolymers 20*, 2583−2621.
Lane, A. N., Jenkins, T. C., Brown, D. J. S., & Brown, T. (1991) *J. Biochem. (Tokyo) 279*, 269−281.
Lavery, R., Zakrzewski, K., & Pullman, B. (1986) *J. Biomol. Struct. Dyn. 3*, 989−1014.
Murray, V., Moore, A. G., Matias, C., & Wickham, G. (1995) *Biochim. Biophys. Acta 1261*, 195−200.
Murray, V., Matias, C., McFadyen, W. D., & Wickham, G. (1996) *Biochim. Biophys. Acta 1305*, 79−86.
Patel, D. J. (1974) *Biochemistry 13*, 2388−2402.
Patel D. J. (1976) *Biopolymers 15*, 533−558.
Prakash, A. S., Moore, A. G., Murray, V., Matias, C., McFadyen, W. D., & Wickham, G. (1995) *Chem.-Biol. Interact. 95*, 17−28.
Reid, B. R., Banks, K., Flynn, P., & Nerdal, W. (1989) *Biochemistry 28*, 1001−1007.
Saenger, W. (1984) in *Principles of Nucleic Acid Structure*, Springer-Verlag, New York.
Scott, E. V., Jones, R. L., Banville, D. L., Zon, G., Marzilli, L. G., & Wilson, W. D.(1988) *Biochemistry 27*, 915−923.
Searle, M. S. (1993) *Prog. Nucl. Magn. Reson. Spectrosc. 25*, 403−480.
Searle, M. S., & Bicknell, W. (1992) *Eur. J. Biochem. 205*, 45−58.
Searle, M. S., Hall, J. G., Denny, W. A., & Wakelin, L. P. G. (1988) *Biochemistry 27*, 4340−4349.
Sun, D., Hansen, M., & Hurley, L. (1995) *J. Am. Chem. Soc. 117*, 2430−2440.
Warshel, A., (1979) *J. Phys. Chem. 83*, 1640−1652.
Weiner, S. J., Kollman, P. A., Case, D. A., Singh, U. C., Ghio, C., Alagona, G., Profeta, S., Jr., & Weiner, P. (1984) *J. Am. Chem. Soc. 106*, 765−784.
Weiner, S. J., Kollman, P. A., Nguyen, D. T., & Case, D. A. (1986) *J. Comput. Chem. 7*, 230−252.
Wemmer, D. E. (1991) *Bull. Magn. Reson. 12*, 185−208.
Wickham, G., Prakash., A. S., Wakelin, L. P. G., & McFadyen, W. D. (1991) *Biochim. Biophys. Acta 1073*, 528−537.
Wickham, G., Iannitti, P., Boschenok, J., & Sheil, M. M. (1995a) *FEBS Lett. 360*, 231−234.
Wickham, G., Iannitti, P., Boschenok, J., & Sheil, M. M. (1995b) *J. Mass. Spectrom.*, S197−S203.
Wüthrich, K. (1986) in *NMR of Proteins and Nucleic Acids* (Wüthrich, K., Ed.) Wiley-Interscience, New York.
Zehnder, M., Séquin, U., & Nadig, H. (1979) *Helv. Chim. Acta 62*, 2525−2533.
Zhang, X., & Patel, D. J. (1990) *Biochemistry 29*, 9451−9466.

BI952542C